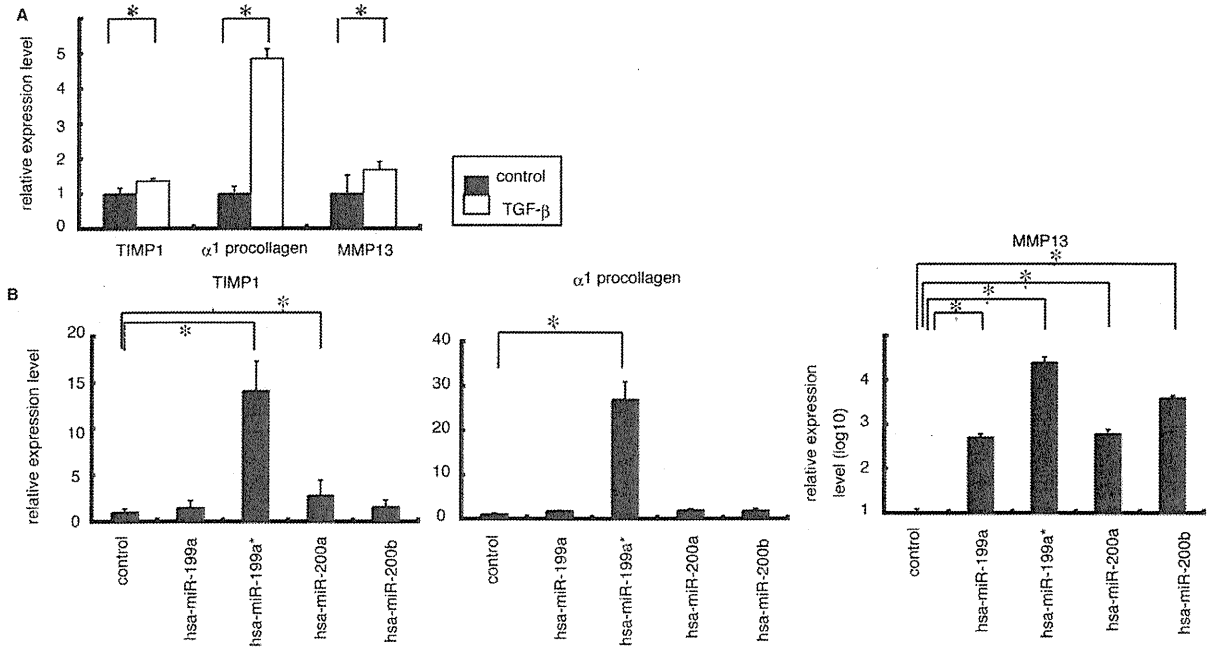

Figure 4. The relationship between expression level of miR-199 and 200 families and expression level of three fibrosis related genes. A. Administration of TGFβ in LX2 cells showed that the expression level of three fibrosis related genes were higher than that in non-treated cells. The data shown are the means+SD of three independent experiments. Asterisk was indicated to the significant difference of $p<0.05$ (two-tailed Student-t test). B. The expression levels of 3 fibrosis related genes in LX2 cells with overexpressing miR-199a, 199a*, 200a, or 200b, respectively were significantly higher than that in cells transfected with control miRNA ($p<0.05$; two-tailed Student t-test).
doi:10.1371/journal.pone.0016081.g004

Moreover miRNA expression profiling has further applications in novel anti-fibrosis therapy in CH.

Materials and Methods

Sample preparation

105 liver tissues samples from chronic hepatitis C patients (genotype 1b) were obtained by fine needle biopsy (Table S1). METAVIR fibrosis stages were F0 in 7 patients, F1 in 57, F2 in 24 and F3 in 17. Patients with autoimmune hepatitis or alcoholic liver injury were excluded. None of the patients were positive for hepatitis B virus associated antigen/ antibody or anti human immunodeficiency virus antibody. No patient received interferon therapy or immunomodulatory therapy prior to the enrollment in this study. We also obtained normal liver tissue from the Liver Transplantation Unit of Kyoto University. All of the patients or their guardians provided written informed consent, and Kyoto University Graduate School and Faculty of Medicine's Ethics Committee approved all aspects of this study in accordance with the Helsinki Declaration.

RNA preparation and miRNA microarray

Total RNA from cell lines or tissue samples was prepared using a *mir*Vana miRNA extraction Kit (Ambion, Austin, TX, USA) according to the manufacturer's instruction. miRNA microarrays were manufactured by Agilent Technologies (Santa Clara, CA, USA) and 100 ng of total RNA was labeled and hybridized using the Human microRNA Microarray Kit protocol for use with Agilent microRNA microarrays Version 1.5 and Mouse microRNA Microarray Kit protocol for use with Agilent microRNA microarrays Version 1.0. Hybridization signals were detected with a DNA microarray scanner G2505B (Agilent Technologies) and the scanned images were analyzed using Agilent feature extraction software (v9.5.3.1). Data were analyzed using GeneSpring GX 7.3.1 software (Agilent Technologies) and normalized as follows: (i) Values below 0.01 were set to 0.01. (ii) In order to compare between one-color expression profile, each measurement was divided by the 75th percentile of all measurements from the same species. The data presented in this manuscript have been deposited in NCBI's Gene Expression Omnibus and are accessible through GEO Series accession number GSE16922 (human) and accession number GSE19865 (mouse).

Real-time qPCR for human miRNA

For detection of the miRNA level by real-time qPCR, TaqMan® microRNA assay (Applied Biosystems) was used to quantify the relative expression level of miR-199a (assay ID. 002304), miR-199a* (assay ID. 000499), miR-200a (assay ID. 000502), miR-200b (assay ID. 002251), and U18 (assay ID. 001204) was used as an internal control. cDNA was synthesized using the Taqman miRNA RT Kit (Applied Biosystems). Total RNA (10 ng/ml) in 5ml of nuclease free water was added to 3 ml of 5× RT primer, 10× 1.5μl of reverse transcriptase buffer, 0.15 μl of 100 mM dNTP, 0.19 μl of RNase inhibitor, 4.16 μl of nuclease free water, and 50U of reverse transcriptase in a total volume of 15 μl. The reaction was performed for 30 min at 16°C, 30 min at 42°C, and 5 min at 85°C. All reactions were run in triplicate. Chromo 4 detector (BIO-RAD) was used to detect miRNA expression.

Animal and Chronic Mouse Liver Injury Model

Each 5 adult (8-week-old) male C57BL/6J mice were given a biweekly intra-peritoneal dose of a 10% solution of CCL_4 in olive oil (0.02 ml/g/ mouse) for the first 4 weeks and then once a week

for the next 4 weeks. At week 4, 6 or 8, the mice were sacrificed. Partial livers were fixed, embedded in paraffin, and processed for histology. Serial liver sections were stained with hematoxylin-eosin, Azan staining, Silver (Ag) staining, and Elastica van Gieson (EVG) staining, respectively. Total RNA from mice liver tissue was prepared as described previously. All animal procedures concerning the analysis of liver injury were performed in following the guidelines of the Kyoto University Animal Research Committee and were approved by the Ethical Committee of the Faculty of Medicine, Kyoto University.

Cell lines and Cell preparation

The human stellate cell lines LX-2, was provided by Scott L. Friedman. LX-2 cells, which viable in serum free media and have high transfectability, were established from human HSC lines [26]. LX-2 cells were maintained in D-MEM (Invitrogen, Carlsbad, CA, USA) with 10% fetal bovine serum, plated in 60 mm diameter dishes and cultured to 70% confluence. Huh-7 and Hela cells were also maintained in D-MEM with 10% fetal bovine serum. HuS-E/2 immortalized hepatocytes were cultured as described previously [27]. LX-2 cells were then cultured in D-MEM without serum with 0.2% BSA for 48 hours prior to TGFβ1 (Sigma-Aldrich, Suffolk, UK) treatment (2.5 ng/ml for 20 hours). Control cells were cultured in D-MEM without fetal bovine serum.

miRNA transfection

LX-2 cells were plated in 6-well plates the day before transfection and grown to 70% confluence. Cells were transfected with 50 pmol of Silencer® negative control siRNA (Ambion) or double-stranded mature miRNA (Hokkaido System Science, Sapporo, Japan) using lipofectamine RNAiMAX (Invitrogen). Cells were harvested 2 days after transfection.

Real-time qPCR

cDNA was synthesized using the Transcriptor High Fiderity cDNA synthesis Kit (Roche, Basel, Switzerland). Total RNA (2 μg) in 10.4 μl of nuclease free water was added to 1 μl of 50mM random hexamer. The denaturing reaction was performed for 10min at 65°C. The denatured RNA mixture was added to 4 μl of 5× reverse transcriptase buffer, 2 μl of 10 mM dNTP, 0.5 μl of 40U/μl RNase inhibitor, and 1.1 μl of reverse transcriptase (FastStart Universal SYBR Green Master (Roche) in a total volume of 20 μl. The reaction ran for 30 min at 50°C (cDNA synthesis), and five min at 85°C (enzyme denaturation). All reactions were run in triplicate. Chromo 4 detector (BIO-RAD, Hercules, CA, USA) was used to detect mRNA expression. The primer sequences are follows; MMP13 s; 5′-gaggctccgagaaatgcagt-3′, as; 5′-atgccatcgtgaagtctggt-3′, TIMP1 s; 5′-cttggcttctgcactgatgg-3′, as; 5′-acgctggtataaggtggtct-3′, α1-procollagen s; 5′-aacatgaccaaaaaccaaaagtg-3′, as; 5′-cattgtttcctgtgtcttctgg-3′, and β-actin s; 5′-ccactggcatcgtgatggac-3′, as; 5′-tcattgccaatggtgatgacct-3′. Assays were performed in triplicate, and the expression levels of target genes were normalized to expression of the β-actin gene, as quantified using real-time qPCR as internal controls.

Statistical analyses

Statistical analyses were performed using Student's *t*-test; *p* values less than 0.05 were considered statistically significant. Microarray data were also statistically analyzed using Welch's test and Bonferroni correction for multiple hypotheses testing.

Supporting Information

Figure S1 Time line of the induction of chronic liver fibrosis. Upward arrow indicated administration of olive oil or CCl_4. Downward arrow indicates when mice were sacrificed.
(TIF)

Figure S2 Comparison of the expression level of miR-199 and 200 familes in several cell lines and human liver tissue. Endogenous expression level of miR-199a, 199a*, 200a, and 200b in normal liver and LX2 cell as determined by microarray analysis (Agilent Technologies). Endogenous expression level of same miRNAs in Hela, Huh-7 and, immortalized hepatocyte: HuS-E/2 by previously analyzed data [9].
(TIF)

Table S1 Clinical characteristics of patients by the grade of fibrosis.
(DOCX)

Table S2 Extracted human miRNAs related to liver fibrosis.
(DOCX)

Table S3 Corresponding human and mouse miRNAs.
(DOCX)

Table S4 Hypothetical miRNA target genes according to in silico analysis.
(DOCX)

Author Contributions

Conceived and designed the experiments: YM KS. Performed the experiments: YM HT YH NK. Analyzed the data: MT MK. Contributed reagents/materials/analysis tools: YM HT YH NK. Wrote the paper: YM MT AT FM NK TO.

References

1. Wasley A, Alter MJ (2000) Epidemiology of hepatitis C: geographic differences and temporal trends. Semin Liver Dis 20: 1–16.
2. Shepard CW, Finelli L, Alter MJ (2005) Global epidemiology of hepatitis C virus infection. Lancet Infect Dis 5: 558–567.
3. Gressner AM, Weiskirchen R (2006) Modern pathogenetic concepts of liver fibrosis suggest stellate cells and TGF-beta as major players and therapeutic targets. J Cell Mol Med 10: 76–99.
4. Nilsen TW (2007) Mechanisms of microRNA-mediated gene regulation in animal cells. Trends Genet 23: 243–249.
5. Zamore PD, Haley B (2005) Ribo-gnome: the big world of small RNAs. Science 309: 1519–1524.
6. Pillai RS (2005) MicroRNA function: multiple mechanisms for a tiny RNA? Rna 11: 1753–1761.
7. Ura S, Honda M, Yamashita T, Ueda T, Takatori H, et al. (2009) Differential microRNA expression between hepatitis B and hepatitis C leading disease progression to hepatocellular carcinoma. Hepatology 49: 1098–1112.
8. Yamamoto Y, Kosaka N, Tanaka M, Koizumi F, Kanai Y, et al. (2009) MicroRNA-500 as a potential diagnostic marker for hepatocellular carcinoma. Biomarkers 14: 529–538.
9. Murakami Y, Yasuda T, Saigo K, Urashima T, Toyoda H, et al. (2006) Comprehensive analysis of microRNA expression patterns in hepatocellular carcinoma and non-tumorous tissues. Oncogene 25: 2537–2545.
10. Jin X, Ye YF, Chen SH, Yu CH, Liu J, et al. (2008) MicroRNA expression pattern in different stages of nonalcoholic fatty liver disease. Dig Liver Dis.
11. Ogawa T, Iizuka M, Sekiya Y, Yoshizato K, Ikeda K, et al. (2009) Suppression of type I collagen production by microRNA-29b in cultured human stellate cells. Biochem Biophys Res Commun.
12. Ji J, Zhang J, Huang G, Qian J, Wang X, et al. (2009) Over-expressed microRNA-27a and 27b influence fat accumulation and cell proliferation during rat hepatic stellate cell activation. FEBS Lett 583: 759–766.
13. Wienholds E, Kloosterman WP, Miska E, Alvarez-Saavedra E, Berezikov E, et al. (2005) MicroRNA expression in zebrafish embryonic development. Science 309: 310–311.

14. Landgraf P, Rusu M, Sheridan R, Sewer A, Iovino N, et al. (2007) A mammalian microRNA expression atlas based on small RNA library sequencing. Cell 129: 1401–1414.
15. Friedman SL (2008) Hepatic fibrosis-Overview. Toxicology.
16. Roderburg C, Urban GW, Bettermann K, Vucur M, Zimmermann H, et al. (2010) Micro-RNA profiling reveals a role for miR-29 in human and murine liver fibrosis. Hepatology.
17. Venugopal SK, Jiang J, Kim TH, Li Y, Wang SS, et al. (2010) Liver fibrosis causes downregulation of miRNA-150 and miRNA-194 in hepatic stellate cells, and their overexpression causes decreased stellate cell activation. Am J Physiol Gastrointest Liver Physiol 298: G101–106.
18. Jiang J, Gusev Y, Aderca I, Mettler TA, Nagorney DM, et al. (2008) Association of MicroRNA expression in hepatocellular carcinomas with hepatitis infection, cirrhosis, and patient survival. Clin Cancer Res 14: 419–427.
19. Jiang X, Tsitsiou E, Herrick SE, Lindsay MA (2010) MicroRNAs and the regulation of fibrosis. Febs J 277: 2015–2021.
20. Marquez RT, Bandyopadhyay S, Wendlandt EB, Keck K, Hoffer BA, et al. (2010) Correlation between microRNA expression levels and clinical parameters associated with chronic hepatitis C viral infection in humans. Lab Invest.
21. Kim S, Lee UJ, Kim MN, Lee EJ, Kim JY, et al. (2008) MicroRNA miR-199a* regulates the MET proto-oncogene and the downstream extracellular signal-regulated kinase 2 (ERK2). J Biol Chem 283: 18158–18166.
22. Murakami Y, Aly HH, Tajima A, Inoue I, Shimotohno K (2009) Regulation of the hepatitis C virus genome replication by miR-199a. J Hepatol 50: 453–460.
23. Gibbons DL, Lin W, Creighton CJ, Rizvi ZH, Gregory PA, et al. (2009) Contextual extracellular cues promote tumor cell EMT and metastasis by regulating miR-200 family expression. Genes Dev 23: 2140–2151.
24. Gregory PA, Bert AG, Paterson EL, Barry SC, Tsykin A, et al. (2008) The miR-200 family and miR-205 regulate epithelial to mesenchymal transition by targeting ZEB1 and SIP1. Nat Cell Biol 10: 593–601.
25. Oberti F, Valsesia E, Pilette C, Rousselet MC, Bedossa P, et al. (1997) Noninvasive diagnosis of hepatic fibrosis or cirrhosis. Gastroenterology 113: 1609–1616.
26. Xu L, Hui AY, Albanis E, Arthur MJ, O'Byrne SM, et al. (2005) Human hepatic stellate cell lines, LX-1 and LX-2: new tools for analysis of hepatic fibrosis. Gut 54: 142–151.
27. Aly HH, Watashi K, Hijikata M, Kaneko H, Takada Y, et al. (2007) Serum-derived hepatitis C virus infectivity in interferon regulatory factor-7-suppressed human primary hepatocytes. J Hepatol 46: 26–36.

MicroRNA-143 Regulates Human Osteosarcoma Metastasis by Regulating Matrix Metalloprotease-13 Expression

Mitsuhiko Osaki[1–3], Fumitaka Takeshita[1], Yui Sugimoto[2], Nobuyoshi Kosaka[1], Yusuke Yamamoto[1], Yusuke Yoshioka[1], Eisuke Kobayashi[4], Tesshi Yamada[4], Akira Kawai[5], Toshiaki Inoue[3], Hisao Ito[6], Mitsuo Oshimura[2,3] and Takahiro Ochiya[1]

[1]Division of Molecular and Cellular Medicine, National Cancer Center Research Institute, Tokyo, Japan; [2]Division of Molecular Genetics and Biofunction, Tottori University Graduate School of Medical Science, Tottori, Japan; [3]Chromosome Engineering Research Center, Tottori University, Tottori, Japan; [4]Division of Chemotherapy and Clinical Reasearch, National Cancer Center Research Institute, Tokyo, Japan; [5]Orthopedics Division, National Cancer Center Hospital, Tokyo, Japan; [6]Division of Organ Pathology, Tottori University, Tottori, Japan

Pulmonary metastases are the main cause of death in patients with osteosarcoma, however, the molecular mechanisms of metastasis are not well understood. To detect lung metastasis-related microRNA (miRNA) in human osteosarcoma, we compared parental (HOS) and its subclone (143B) human osteosarcoma cell lines showing lung metastasis in a mouse model. miR-143 was the most downregulated miRNA ($P < 0.01$), and transfection of miR-143 into 143B significantly decreased its invasiveness, but not cell proliferation. Noninvasive optical imaging technologies revealed that intravenous injection of miR-143, but not negative control miRNA, significantly suppressed lung metastasis of 143B ($P < 0.01$). To search for miR-143 target mRNA in 143B, microarray analyses were performed using an independent RNA pool extracted by two different comprehensive miR-143-target mRNA collecting systems. Western blot analyses revealed that MMP-13 was mostly protein downregulated by miR-143. Immunohistochemistry using clinical samples clearly revealed MMP-13-positive cells in lung metastasis-positive cases, but not in at least three cases showing higher miR-143 expression in the no metastasis group. Taken together, these data indicated that the downregulation of miR-143 correlates with the lung metastasis of human osteosarcoma cells by promoting cellular invasion, probably via MMP-13 upregulation, suggesting that miRNA could be used to develop new molecular targets for osteosarcoma metastasis.

Received 28 December 2010; accepted 22 February 2011; published online 22 March 2011. doi:10.1038/mt.2011.53

INTRODUCTION

Osteosarcoma is the most common primary bone malignancy and accounts for 60% of all malignant childhood bone tumors.[1] The age distribution is bimodal: the first major peak occurring during the second decade of life, and the second much smaller peak being observed in patients over 50 years of age. The distal femoral and proximal tibial metaphyses are the most common sites for osteosarcoma. Approximately 50% of cases are localized in the knee region.[2] With combined treatment (neoadjuvant chemotherapy, surgery, and adjuvant chemotherapy), the 5-year survival of patients with no metastatic disease at diagnosis is 60–70%;[3–5] however, for patients who present with metastatic disease, the outcome is far worse at <30% survival.[6] Pulmonary metastasis is the predominant site of osteosarcoma recurrence and the most common cause of death. Unfortunately, survival has not improved for 20 years despite multiple clinical trials with increased intensity, and further gains with refinements of cytotoxic chemotherapy regimens alone are unlikely; therefore, for better prognosis, new therapeutic targets and approaches must be sought to suppress pulmonary metastasis of osteosarcoma.

MicroRNA (miRNA) belongs to a class of endogenously expressed, non-coding small RNA and contains about 22 nucleotides. Based on miRBase release 16.0, >1,000 human miRNA have been registered with a large number being evolutionarily conserved.[7] It has been shown that miRNA can regulate the expression of protein-coding genes at the post-transcriptional level through imperfect base pairing with the 3′-untranslated region (3′-UTR) of target mRNA.[8] miRNA is predicted to regulate the expression of at least 30% of all genes.[9] Growing evidence suggests that deregulation of miRNA may contribute to many types of human diseases, including cancer. Errors in the expression of miRNA have been observed in various types of cancers[10,11] and are also associated with the clinical outcome of cancer patients.[12,13] Consistently, miRNA has been implicated in the regulation of various cellular processes that are often deregulated during tumor development and progression,[8,14–17] suggesting that miRNA might be a target for cancer therapy.

The most direct way for molecules to correct altered miRNA expression is by treatment with RNA oligonucleotides. Therapeutic potentials using RNA oligonucleotides have been proposed, although our understanding of the role of miRNA in cancer is still very limited. There are two possible approaches: blocking oncogenic

Correspondence: *Mitsuhiko Osaki, Division of Molecular Genetics and Biofunction, Tottori University Graduate School of Medical Science, 86 Nishi-cho, Yonago, Tottori 683–8503, Japan. E-mail: osamitsu@med.tottori-u.ac.jp*

© The American Society of Gene & Cell Therapy

miRNA by anti-miRNA oligonucleotides or replacement of miRNA with tumor suppressor activity by miRNA mimetics. In fact, *in vitro* studies have revealed that anti-miR-17-5p treatment halts the growth of a human neuroblastoma cell line, LAN-5, overexpressing miR-17-5p.[18] Si *et al.* also reported that anti-miR-21 inhibited cell growth via increased apoptosis and decreased cell proliferation, which could partly be due to the downregulation of antiapoptotic Bcl-2 in a human breast cancer cell line, MCF-7.[19] Recently, Ma *et al.* reported that systemic administration of miR-10b antagomir inhibited lung metastasis of mouse breast cancer cells in a mouse model.[20] On the other hand, it has been reported that cell proliferation or invasion was suppressed by miRNA mimetics transfection into human cancer cells. For example, the introduction of synthesized miR-143 or miR-145 into a human B-cell lymphoma cell line, Raji, resulted in significant growth inhibition that occurred in a dose-dependent manner.[21] Crawford *et al.* reported that treatment with miR-126 decreased adhesion, migration, and the invasion of a human nonsmall-cell lung carcinoma cell line, H1703.[22] Valastyan *et al.* found that overexpression of miR-31 independently inhibited the invasive capacity of MDA-MB-231 breast cancer cells, extravasation into or survival in the lung parenchyma, and metastatic colonization.[23] Moreover, Tazawa *et al.* demonstrated in a mouse model that direct intratumoral injection of a miR-34a/atelocollagen complex successfully suppressed the growth of tumors derived from human colon cancer cells.[24] Furthermore, significant reduction of the tumor volume was observed until day 6 after miR-34a administration. Interestingly, the authors showed that the expression of miR-34a was downregulated in more than one-third of human colon cancers compared with counterpart normal colon mucosa. Therefore, these data suggested that restoring decreased miRNA in cancer cells was able to suppress the progression of cancer *in vivo*.

Our goal is to understand the mechanisms of metastases and, based on this knowledge, identify new targets that can be used for the development of new molecular markers and therapeutic approaches to inhibit metastasis from osteosarcoma. In this study, we explored miRNA and its target mRNA associated with cell invasion of osteosarcoma cells *in vitro* using two human osteosarcoma cell lines, HOS and 143B, and aimed to clarify whether spontaneous lung metastasis from osteosarcoma could be suppressed by restoring or blocking miRNA *in vivo* using a mouse model.

RESULTS

miRNA microarray analysis and validation of the array data by real-time RT-PCR

Two human osteosarcoma cell lines, HOS and 143B, were used to discover metastasis-related miRNA candidates. The 143B line was generated by transformation of HOS via v-Ki-ras and, unlike HOS, demonstrated high tumorigenecity and spontaneous metastatic potential after orthotopic intratibial inoculation.[25] Thus, by comparing the miRNA expression patterns of these cells, it is suggested that metastasis-related miRNA is extractable. miRNA microarray analysis was performed comparing HOS and 143B cells to evaluate the miRNA profiles of each cell. It was observed that the expression of many miRNAs in the two cell lines was different. Nineteen miRNAs were significantly upregulated, whereas nine miRNAs, including miR-143, were significantly downregulated in 143B compared to HOS (Table 1). It was suggested that the former were metastasis-promoting miRNA and the latter were metastasis-suppressing miRNA.

By miRNA microarray analysis, miR-143 was decreased about 1/10 as compared to HOS. Based on the microarray results, we examined the expression level of miR-143 with real-time reverse transcriptase (RT)-PCR. For that purpose, RNA pooled from the same RNA samples used for the microarray experiments was prepared. Additionally, we determined *RNU6B* as a reference gene for normalization of miRNA data. The PCR result was consistent with the microarray data because miR-143 was downregulated less than one-tenth the level in 143B (**Supplementary Figure S1**).

miRNA mimic or anti-miRNA oligonucleotide transfer allows efficient inhibition of 143B-luc cell invasion, but not proliferation, *in vitro*

To screen target genes showing inhibition of invasion in 143B cells transfected with firefly luciferase gene (*143B-luc*), the nine most strongly up- and downregulated miRNAs (miRNAs above dotted line in Table 1) were selected for *in vitro* screening (see Materials and Methods section). For monitoring cell invasion and proliferation, we analyzed luciferase activity. As shown in Figure 1, inhibition of cell invasion was significantly ($P < 0.05$) observed on 143B-luc cells transfected with miR-143, followed by miR-145 (not significant). No other miRNA mimics or anti-miRNA inhibited cell invasion in 143B-luc cells. On the other hand, no miRNA

Table 1 Significantly aberrant expression of miRNAs in 143B compared to HOS

Upregulated miRNA		Downregulated miRNA	
Name	Ratio (143B/HOS)	Name	Ratio (143B/HOS)
miR-584	N.D.[a]	miR-143	0.11
miR-146a	N.D.[a]	miR-145	0.12
miR-31	>10	miR-193b	0.15
miR-100	5.09	miR-28	0.28
miR-125b	5.07	miR-149	0.55
miR-222	4.85	miR-99b	0.58
miR-221	4.62	miR-133b	N.D.[b]
miR-29b	4.59	miR-140	N.D.[b]
miR-625	4.57	miR-335	N.D.[b]
miR-29a	4.30		
miR-21	3.62		
miR-148a	3.25		
miR-34a	2.99		
miR-652	2.70		
miR-361	2.48		
miR-210	2.47		
miR-374	2.46		
miR-455	2.20		
miR-23a	2.15		

Abbreviation: miRNA, microRNA.
[a]Not determined, because expression of the miRNA in HOS could not be detected by miRNA microarray analysis. [b]Not determined, because expression of the miRNA in 143B could not be detected by miRNA microarray analysis.

© The American Society of Gene & Cell Therapy

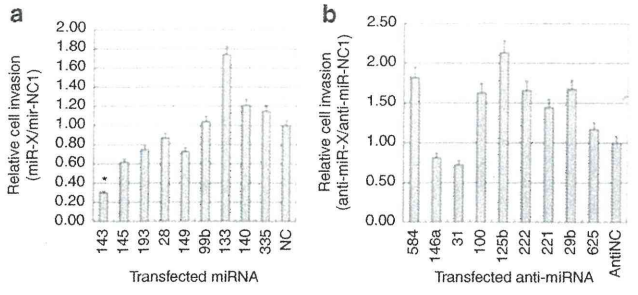

Figure 1 Matrigel invasion assay. The matrigel invasion assay was performed using a human osteosarcoma cell line (143B-luc) transfected with either synthetic (**a**) microRNA (miRNA) or (**b**) anti-miRNA, which were differentially expressed in 143B compared to HOS. Invaded cells were lysed and then analyzed for luciferase activity using the Bright-Glo Luciferase Assay System. Inhibition of luciferase production was normalized to the level of negative control pre-miR- (miR-NC1)- or anti-miR (anti-miR-NC)-transfected cells. The experiment was performed in triplicate and repeated three times. *$P < 0.05$ versus control.

mimics or anti-miRNA used in this assay significantly affected cell proliferation (**Supplementary Figure S2**). These results revealed that miR-143 might be the miRNA with the most potential to suppress the metastasis of 143B-luc cells.

Suppression of spontaneous lung metastasis of osteosarcoma cells in mice with systemic miR-143 treatment

First, we determined the ability of 143B cells transfected with firefly luciferase gene (*143B-luc*) to develop a primary tumor and spontaneous lung metastasis in athymic mice ($n = 10$). Experimentally, 1.5×10^6 143B-luc cells were inoculated into the right knee, and we checked their location immediately after inoculation using an *in vivo* imaging system (IVIS) (**Supplementary Figure S3a**). Subsequently, we checked the inoculated animals weekly for luciferase bioluminescence by IVIS to monitor tumor growth and to visualize the presence of distant metastases in the animals. At 1 week after inoculation, primary tumors were macroscopically detectable in some mice, but no signals were detected in the pulmonary area. At 2 weeks, we observed the first sign of metastasis in some of the mice by IVIS (**Supplementary Figure S3b**). During the subsequent week, numerous metastases could be detected by IVIS. At 4 weeks after tumor cell inoculation, all animals showed signals in the pulmonary area by IVIS and they were sacrificed for histological examination. Many nodules were seen on the surface of the resected lungs (**Supplementary Figure S3c**), and they were confirmed microscopically as osteosarcoma metastatic lesions (**Supplementary Figure S3d**).

To assess the therapeutic potential of miR-143 against spontaneous lung metastasis of osteosarcoma, 50 μg miR-143 mimic or miR-negative control 1 (NC1) mixed with atelocollagen was administered intravenously into mice in each group ($n = 10$ each) at 1, 4, 7, 10, 13, 16, and 19 days after inoculation of 143B-luc cells. The development of a primary tumor and metastasis in the pulmonary area was monitored weekly by IVIS. At 1 week, the signal from firefly luciferase was detected at only the primary lesion in each group (**Figure 2a**). At 2 weeks, 4 of the 10 mice injected with miR-NC1 showed a signal from luciferase in the pulmonary area,

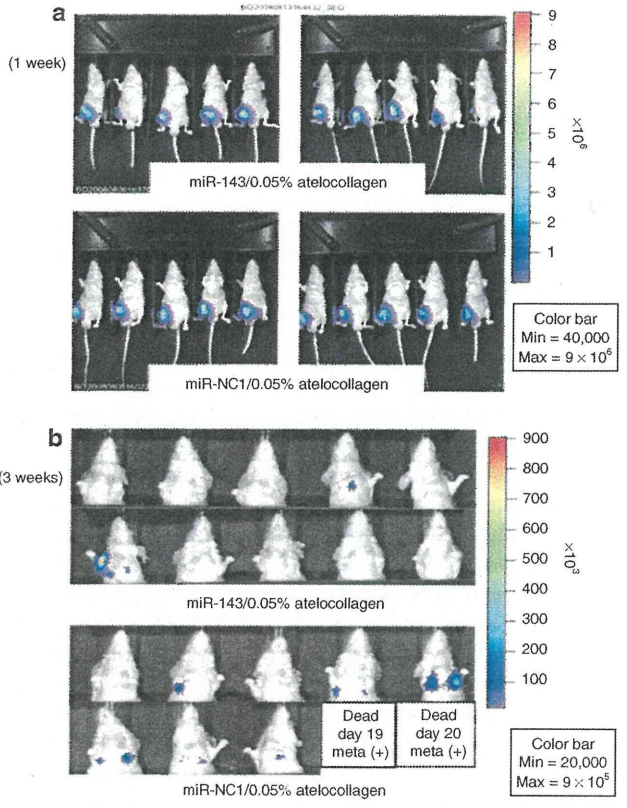

Figure 2 Inhibition of lung metastasis of osteosarcoma by systemic treatment of miR-143. All mice used in this experiment are shown. Luminescence was observed at only the right knee where 143B-luc cells were inoculated at (**a**) 1 week after inoculation. (**b**) At 3 weeks after inoculation, six of eight mice exhibited lung metastasis by *in vivo* imaging system (IVIS) and the other two mice died due to lung metastasis on day 19 and 20, respectively, in miR-NC1/atelocollagen-treated mice, whereas only 2 of the 10 mice in the miR-143/atelocollagen-treated group showed lung metastasis.

suggesting lung metastasis, but no signal was detected in the miR-143-injected mouse group. At days 19 and 20, 2 of the 10 mice in the miR-NC1 group died and lung metastasis was confirmed by autopsy. At 3 weeks, lung metastasis was detected by IVIS in 6 of the 8 live mice (miR-NC1 group). Interestingly, only 2 of the 10 mice injected with miR-143 showed lung metastasis (**Figure 2b**), a significant difference ($P < 0.01$).

To know whether the inhibitory effect of miR-143 on lung metastasis was not due to the direct inhibition of tumor growth in the primary tumor, all mice were sacrificed and the resected primary tumors were examined (**Supplementary Figure S4**). The weight (mean ± SD) of the primary tumor was 3.67 ± 0.59 g (miR-NC1-treated group) and 3.32 ± 0.65 g (miR-143-treated group), respectively, indicating that there were no differences between the two groups. Moreover, the expression of proliferative cell nuclear antigen in the primary tumor was examined by immunohistochemistry. Proliferative cell nuclear antigen-positive cells were observed in most of the tumor cells and no difference was shown between the two groups. These data suggested that miR-143 did not affect tumor growth in the primary lesion during the course of miRNA treatment.

© The American Society of Gene & Cell Therapy

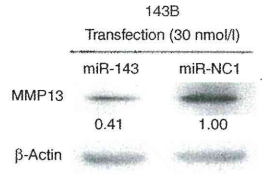

Figure 3 Downregulation of MMP-13 expression by miR-143. Western blot analyses of MMP-13 expression in 143B cells 48 hours after transient transfection of miR-143 or miR-NC1. Relative expression, quantified by Image J software is normalized to β-actin, and measured by the ratio of the indicated situation to miR-NC1.

Detection and identification of *miR-143* target genes

To elucidate metastasis-related *miR-143* target genes in 143B cells, candidate mRNA regulated by miR-143 was comprehensively collected by two different methods, anti-Ago2 antibody immunoprecipitation (Ago2 IP) and the labeled miRNA pull-down (LAMP) assay system (see Materials and Methods section). The collected RNA was validated by microarray analyses and 1,113 genes and 1,658 genes were detected, at least a 1.1-fold increase in miR-143 by Ago2 IP and LAMP, respectively. Of these, 78 genes were commonly detected by both methods (**Supplementary Table S1**). Furthermore, candidate target genes were selected using two criteria: (i) genes that were included in at least one of three publicly available databases, TargetScanHuman 5.1, PicTar, and miranda (September 2008 release) as miR-143 target genes, or (ii) genes that were involved in cell invasion or migration. Six genes met at least one of the two requirements (**Supplementary Table S2**). Western blot analyses revealed that the expression of MMP-13 was suppressed most in the six genes (**Figure 3** and **Supplementary Figure S5**).

Expression of miR-143 and MMP-13 in clinical samples

Finally, we evaluated the expression of miR-143 in human primary osteosarcoma in order to examine whether miR-143 expression there correlated with metastasis. Twenty-two biopsy samples of primary osteosarcoma without any metastases at first diagnosis were analyzed for the expression level of miR-143 by real-time RT-PCR. Seven of the 22 cases showed lung metastasis after resection of the primary tumor, and the other cases (n = 15) showed no metastasis for at least >1 year after the operation. The miR-143 expression data were normalized to the mean of miR-103, which was found to be among the most stably expressed miRNA in human tumor tissues.[26] Three of the fifteen lung metastasis-negative cases showed an extremely higher expression of miR-143, whereas this expression was low in the seven cases that had lung metastasis after the operation (**Figure 4**). The relative expressions of miR-143 were 0.61 ± 0.12 (lung metastasis-positive group) and 1.23 ± 0.43 (no metastasis group). These data suggested that a lower expression of miR-143 in osteosarcoma might tend to occur in lung metastasis, although the difference was not statistically significant between these groups (P = 0.19). MMP-13 expression was evaluated by immunohistochemistry. Five of the seven lung metastasis-positive cases and fourteen of the fifteen lung metastasis-negative cases were available for immunohistochemical examination. As shown in **Figure 4**, MMP-13-positive tumor cells were studded in all of

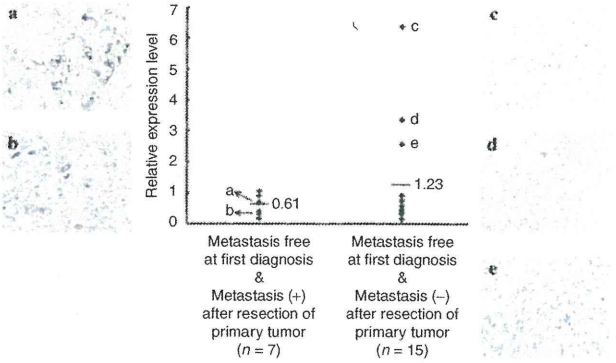

Figure 4 Expression of miR-143 in primary osteosarcoma tissue samples. Twenty-two primary osteosarcoma specimens were divided into two groups: metastasis-positive cases after resection of primary tumor (n = 7, left) and metastasis-free cases at least 1 year after resection of primary tumor (n = 15, right). miR-143 was measured by real-time reverse transcription (RT)-PCR. Individual data are the mean of triplicate measurements from single RNA samples. The expression level of miR-143 is normalized to miR-103. P-values were calculated using Welch's t-test. The mean value for each data set is shown as a horizontal line. MMP-13-positive tumor cells appeared in cases in the lung metastasis-positive group and showed (**a**,**b**) lower miR-143 expression. (**c**–**e**) On the other hand, no positive tumor cells were observed in three cases showing higher miR-143 expression in the lung metastasis-negative group. Each case (**a**–**e**) of dot data is consistent with the case indicated by immunohistochemistry data, respectively.

the five lung metastasis-positive cases (**Figure 4a,b**), whereas only five of the fourteen lung metastasis-negative cases showed MMP-13-positive cells. In other words, expression of MMP-13 in tumor cells was extremely low in 9 of the 14 lung metastasis-negative cases; in particular, no positive tumor cells were observed in three cases showing a higher expression of miR-143 (**Figure 4c–e**).

DISCUSSION

Altered expression of miRNA has recently been reported to impact human carcinogenesis and cancer progression.[10,11,27] In the present study, we found differentially expressed miRNA by comparing 143B and HOS cells, which resemble each other genetically, but showed different phenotypes of metastasis *in vivo*: inoculation of 143B cells, but not HOS cells, into a knee joint led to spontaneous lung metastasis in the athymic mice used in this study, as well as in a previous report.[25] It was considered that metastasis-promoting miRNA was upregulated and/or metastasis-suppressor miRNA was downregulated in 143B cells. Of these miRNAs, we found miR-143 to be the most downregulated miRNA in 143B cells by miRNA microarray analysis. Because cell invasion was inhibited by restoring miR-143 in 143B cells, we injected miR-143 with atelocollagen into spontaneous lung metastasis of an osteosarcoma mouse model to evaluate whether this miRNA could suppress lung metastasis from a primary tumor. Atelocollagen is a biomaterial with potential for use as a carrier for gene delivery.[28] We previously reported that a human enhancer of zeste homolog 2 (EZH2) and human phosphoinositide 3′-hydroxykinase p110α subunit (p110α) small interfering RNA–atelocollagen complexes administered intravenously into mice having a bone metastatic lesion of human prostate cancer markedly suppressed tumor growth in the lesion with no side effect caused by the atelocollagen.[29]

© The American Society of Gene & Cell Therapy

Recently, we also reported that systemic administration of miR-16 with atelocollagen successfully regressed prostate cancer in a bone metastatic lesion in a mouse model.[30] Thus, for prevention of lung metastasis from osteosarcoma, a new atelocollagen-mediated systemic delivery method could be a reliable and safe approach to achieve maximal function of miRNA *in vivo*, as well as small interfering RNA. In the present study, systemic administration of miR-143 with atelocollagen surprisingly suppressed lung metastasis in a spontaneous lung metastatic mouse model. On the other hand, treatment with miR-143 did not affect tumor growth in a primary lesion in an *in vivo* model. These data are consistent with *in vitro* data demonstrating that miR-143 transfection into 143B cells could suppress cell invasion but not cell proliferation, suggesting that miR-143 might specifically regulate the invasion and/or migration signal pathway(s) of osteosarcoma cells.

New approaches that can complement and improve on current strategies for the prediction of prognosis are urgently needed. Many independent studies on different tissues have demonstrated that miRNA expression patterns correlated with the prognosis of cancer patients,[17,31] which generally depends upon the occurrence of metastasis, because ~90% of deaths from solid tumors are caused by metastasis. Therefore, the expression of miRNA that regulate cell adhesion, migration and invasion could be a good diagnostic marker to predict cancer prognosis. Ma *et al.* reported that miR-10b is highly expressed in metastatic breast cancer cells and positively regulates cell migration and invasion,[32] and they also demonstrated that systemic administration of miR-10b antagomir inhibited lung metastasis of mouse breast cancer cells in a mouse model.[20] Overexpression of miR-10b in otherwise nonmetastatic breast tumors initiates robust invasion and metastasis. Expression of miR-10b is induced by the transcription factor Twist, which is an epithelial-mesenchymal transition factor and is known to bind directly to the putative promoter of miR-10b. The miR-10b induced by twist inhibits translation of the mRNA encoding homeobox D10, resulting in increased expression of a well-characterized prometastatic gene, *RhoC*. Significantly, the level of miR-10b expression in primary breast carcinomas correlates with clinical progression. On the other hand, Tavazoie *et al.* showed that restoring the expression of miR-335 in a human breast cancer cell line MDA-MB-231 inhibited metastatic cell invasion.[33] miR-335 suppresses metastasis and migration through targeting of the progenitor cell transcription factor SOX4 and extracellular matrix component tenascin C. Moreover, the expression of miR-335 is downregulated in the majority of primary breast tumors from patients who relapse, and hence loss of the expression of miR-335 is associated with poor distal metastasis-free survival. These reports suggested that altered expression of metastasis-associated miRNA could be used for the prediction of prognosis. In the present study, expression analysis of miR-143 using clinical osteosarcoma samples showed that the mean of the expression level was two times higher in metastasis-free cases than in metastasis-positive cases. However, no statistical significance was shown, which might be because only three cases that showed a higher expression of miR-143 raised the mean in metastasis-free cases. In other words, however, it could be considered that osteosarcoma in which a relatively higher level of miR-143 is expressed might be considered a low risk for metastasis. It is suggested that the expression level of miR-143 at a primary osteosarcoma lesion might be a prognostic marker for lung metastasis.

It has been reported that reduced expression of tumor-suppressor miRNA was caused by chromosome deletions, epigenetical changes, abberant transcription, and disturbances in miRNA processing. Suzuki *et al.* reported that P53 enhances the post-transcriptional maturation of several miRNAs, including miR-143. P53 interacts with Drosha processing complex through association with DEAD-box RNA helicase p68. Thus, wild-type P53 could facilitate the processing of primary miR-143 to precursor miR-143, but mutated P53 interferes with functional assembly between Dorosha complex and P68, leading to attenuation of miR-143 processing activity in HCT116, a human colon cancer cell line.[34] Another study showed that upregulation of KRAS leads to downregulation of miR-143 in human pancreatic cancer cell lines;[35] however, the mechanism of this downregulation has not been investigated in osteosarcoma cells in detail. Thus, further studies are needed to reveal the precise mechanism of miR-143 downregulation in 143B cells. The downregulation of miR-143 expression was also reported in several human cancers, e.g., colorectal cancer,[36] prostate cancer,[37] cervical cancer,[38] ovarian cancer,[39] B-cell lymphoma;[21] thus, it is considered that miR-143 is a tumor-suppressor miRNA. In these cancers, downregulation of miR-143 resulted in the promotion of cell proliferation or inhibition of apoptosis, indicating that miR-143 acts as a suppressor on cell proliferation and viability. Akao *et al.* reported that the target gene of miR-143 was determined to be ERK5/MAPK7, the upregulation of which leads to cell growth via activation of c-Myc, in Raji cells, a human B-cell lymphoma cell line.[21] Recently, another paper showed that miR-143 suppressed cell proliferation by inhibiting KRAS translation in human colorectal cancer;[40] however, our data showed that restoring miR-143 in human osteosarcoma cell 143B could suppress cell invasion, but not cell proliferation in *in vitro* and *in vivo* studies. Also, western blotting showed that the expression levels of KRAS and ERK5 did not change by transfecting miR-143 into 143B cells (**Supplementary Figure S6**). These data suggested that miR-143 might have different targets in a cell-type-dependent manner. Additionally, Tome *et al.* reported that *in vivo* transfer of the *KRAS* gene from high-metastatic cancer cells to coimplanted low-metastatic cancer cells enhanced lung metastasis of human osteosarcoma cells,[41] indicating that KRAS is a key factor in the metastasis of osteosarcoma cells; however, our data showed that miR-143 could suppress lung metastasis of 143B cells without KRAS downregulation. Therefore, this might also indicate that miR-143-target genes play roles downstream of the KRAS-related metastasis-promoting pathway(s).

To find which targets are regulated by miR-143 in 143B cells, microarray analyses were performed after collecting target RNA by two independent comprehensive methods (Ago2 IP and LAMP), respectively. By extracting the common genes after the two different collection methods, 78 common genes were identified in >1,000 genes. Of those, six genes matched the requirements of (i) predicted genes by database (Target Scan, PicTar, or miRanda) or (ii) genes related to migration, invasion, or metastasis. Interestingly, protein expressions of at least four of the six genes were downregulated by miR-143 transfection in 143B cells, indicating that the miRNA-target gene detection system in the

present study is a very powerful tool to identify real target genes in each cell line. Our data revealed that MMP-13 was the most downregulated protein by miR-143 in these target genes.

MMP-13 is a proteolytic enzyme that belongs to a large family of extracellular matrix-degrading endopeptidases that are characterized by a zinc-binding motif at their catalytic sites, and the overexpression of MMP-13 has been documented in squamous cell carcinoma of head and neck,[42] lung,[43] malignant melanoma,[44] and colorectal[45] cancer. The expression in these human cancers was associated with cell cancer progression, including invasion and metastasis, diagnosis or poor outcome. In the present study, immunohistochemical analyses using clinical samples revealed that three cases expressing higher miR-143 showed few positive cells of MMP-13 in the primary lesion and all three cases were in the non-metastatic group. On the other hand, MMP-13-positive sarcoma cells were strongly or moderately observed in all lung metastasis-positive cases. These data suggested that downregulation of miR-143 led to upregulation of MMP-13 expression in human osteosarcoma cells and contributed to facilitation of lung metastasis from the primary lesion; therefore, delivering miR-143 mimic into tumor cells could prevent lung metastasis of human osteosarcoma by suppressing at least MMP-13 expression. Because a single miRNA can potentially target many mRNAs, not only MMP-13 but also the other candidate genes identified, as shown in **Supplementary Table S2**, might be involved in metastatic regulation directly or indirectly in 143B cells. Thus, it is possible that interaction of these gene products resulted in positive regulation of cell migration and/or invasion of osteosarcoma cells, and such a mechanism might be negatively regulated by miR-143 as a whole.

In conclusion, we have identified miR-143 as a metastasis-suppressive miRNA of human osteosarcoma cells and demonstrated that systemic administration of miR-143 with atelocollagen into cancer model mice was able to suppress spontaneous lung metastasis of osteosarcoma. To our knowledge, our results present the first evidence that systemic injection of miRNA/atelocollagen complexes may have therapeutic potential for the prevention of lung metastasis from osteosarcoma, although further extensive studies will be required to demonstrate the long-term efficacy and safety of nucleic acid treatment in various *in vivo* experiments. Finally, we successfully identified *MMP-13* and several other genes as probable candidates of miR-143 using a comprehensive collection system to detect miRNA-target mRNA. This system would be a powerful tool to identify single miRNA-target mRNA in a cell- or tissue-specific manner, and might contribute to reveal the mechanism of cancer generation and progression in the point of miRNA functions.

MATERIALS AND METHODS

Cell lines. Two human osteosarcoma cell lines (HOS and 143B) were obtained from the American Type Culture Collection and maintained in Dulbecco's modified Eagle's medium containing 10% heat-inactivated fetal bovine serum. The 143B cell line was generated via Kirsten mouse sarcoma virus (Ki-ras$^+$) transformation of the HOS cell line. The 143B cells were transfected with a complex of pLuc-Neo plasmid DNA (Clontech, Palo Alto, CA) and DharmaFECT (GE Healthcare, Little Chalfont, UK) in accordance with the manufacturers' instructions. Stable transfectants were selected in geneticin (600 μg/ml; Invitrogen, Carlsbad, CA). Clones expressing the luciferase gene were named *143B-Luc*.

Clinical sample. Twenty-two biopsy samples of human osteosarcomas, which did not have metastasis in the lung and other organs at first diagnosis, were obtained from the National Cancer Center Hospital. All the materials were obtained with written informed consent, and the procedures were approved by the institutional review board.

RNA extraction and quantitative real-time PCR of miRNAs. Total RNA was extracted from cell lines and clinical samples using the mirVana miRNA Isolation Kit (Ambion, Austin, TX) according to the manufacturer's protocol.

miR-143-specific complementary DNA was generated from 20 ng total RNA using the TaqMan MicroRNA RT kit (Applied Biosystems, Foster City, CA) and the miR-143-specific RT-primer from the TaqMan Micro RNA Assay (Applied Biosystems). miR-143 levels were also measured using the miR-143-specific probe included with the TaqMan Micro RNA Assay on a Real-Time PCR System 7300 and SDS software (Applied Biosystems).

miRNA microarray analysis. miRNA microarrays were manufactured by Agilent Technologies (Santa Clara, CA), and contain 470 human miRNAs [Agilent Technologies (http://www.chem.agilent.com/scripts/PHome.asp)]. Four independently extracted RNA samples were used for array analyses in each cell line. Labeling and hybridization of total RNA samples were performed according to the manufacturer's protocol. Microarray results were extracted using Agilent Feature Extraction software (v9.5.3.1) and analyzed using Gene- Spring GX 7.3.1 software (Agilent Technologies).

Transfection with synthetic miRNA and assays of cell proliferation and invasion. Synthetic has-miRs (pre-miR-hsa-miR-143, -145, -193b, -28, -149, -99b, -133, -140, -335 and negative control 1 (NC1; Ambion) or hsa-anti-miRs (Anti-miR-hsa-miR-584, -146, -31, -100, -125b, -222, -221, -29b, -625 and negative control; Ambion) were transfected into 143B-Luc cells at 30 nmol/l each (final concentration) per 1×10^6 cells/well of a 6-well plate using DharmaFECT (GE Healthcare). After 48 hours of incubation, cells were harvested and reseeded into a 96-well plate. Pre-miR- or anti-miR-transfected cells were plated at 1×10^4 cells/well in a 96-well plate and incubated for 4 days for the cell proliferation assay. The cell invasion assay was performed using CytoSelect 96-Well Cell Invasion Assay (Cell Biolabs, San Diego, CA). Pre-miR- or anti-miR-transfected cells were plated at 1×10^5 cells/well in 96-well chambers. The protocol followed the manufacturer's instructions (Cell Biolabs). Bioluminescence from 143B-Luc cells highly correlated to the total number of cells.[46] For monitoring the inhibition of cell proliferation or invasion, the cells were lysed ($n = 3$) and then analyzed for luciferase activity (Bright-Glo Luciferase Assay System; Promega, Madison, WI). Inhibition of luciferase production was normalized to the level of negative control Pre-miR- or anti-miR-transfected cells.

Animal model. Animal experiments in the present study were performed in compliance with the guidelines of the Institute for Laboratory Animal Research, National Cancer Center Research Institute. Five- to six-week-old male athymic nude mice (CLEA Japan, Shizuoka, Japan) were anesthetized by exposure to 3% isoflurane on day 0 and subsequent days. On day 0 of the experiments, to generate an experimental model, the anesthetized animals were injected with 1.5×10^6 143B-Luc cells into the right knee.[47,48]

Preparation of complex with miR-143 and atelocollagen. To prepare complexes of miRNA and atelocollagen (Koken, Tokyo, Japan), equal volumes of atelocollagen (0.1% in phosphate-buffered saline at pH 7.4) and miRNA solution were combined and mixed by rotating for 1 hour at 4 °C. The final concentration of atelocollagen was 0.05%.

Evaluation of miR-143/atelocollagen administration into spontaneous lung metastasis of osteosarcoma model mouse. One day after the 143B-Luc cell injection as above, individual mice were injected with 200 μl atelocollagen containing 50 μg miR-143 or miR-NC1 via the tail vain. miRNA/

© The American Society of Gene & Cell Therapy

atelocollagen complexes were injected on days 1, 4, 7, 10, 13, 16, 19, 22, and 25 postinoculation of 143B-Luc cells. Each experimental condition included 10 animals/group. For *in vivo* imaging, the mice were injected with D-luciferin (150 mg/kg; Promega) by intraperitoneal injection. Ten minutes later, photons from firefly luciferase were counted using the IVIS imaging system (Xenogen, Alameda, CA) according to the manufacturer's instructions. Data were analyzed using LivingImage software (version 2.50; Xenogen). The development of subsequent lung metastasis was monitored once a week *in vivo* by bioluminescent imaging for 4 weeks. At the end of the experiment on day 28, the primary tumor and lung of each animal were resected at necropsy for histological analysis.

Comprehensive collection and identification of miR-143 target mRNAs in 143B cells. We used two experimental approaches, immunoprecipitation of RNA-induced silencing complex by anti-Ago2 antibody (Ago2 IP) and the labeled miRNA pull-down (LAMP) assay system, to collect comprehensive target genes of miR-143. In the former method, after transfection of miR-143 or miR-NC1 into 143B, RNA-induced silencing complex was immunoprecipitated by the miRNA isolation kit, human Ago2 (Wako, Osaka, Japan) and RNA was isolated by mirVana (Ambion). The latter method, the LAMP assay system, was performed according to a previous report.[49] Briefly, cell lysate was prepared by an ultrasonic processor (Sonifier 250; Sonifier, Branson, CT) at duty cycle: 20% and output control: 1 with an interval of 30 seconds for 10 times on ice from 5 to 10×10^6 143B cells. After sonication, cell lysate was centrifuged at 15,600*g* for 30 minutes at 4 °C, and the clear cell extract was collected. Next, the pre-miR-143 sequence was amplified by PCR and then subcloned into the pSPT19 (Roche Diagnostics K.K., Tokyo, Japan). Digoxigenin-labeled pre-miR-143 or pre-miR-NC1 was transcribed by the digoxigenin RNA labeling kit (Roche), and then mixed with cell extracts. Next, this digoxigenin-labeled miRNA processed by Dicer *in vitro* was attached to its target genes by endogenous RNA-induced silencing complex. The mixtures of miRNA-target mRNA were then pulled down by anti-digoxigenin monoclonal antibody (1.71.256; Roche) and RNA was isolated by mirVana (Ambion). Finally, the isolated mRNA was reverse-transcribed to complementary DNA and 3D-Gene Human Oligo chip 25k (Toray Industries, Tokyo, Japan) was used to analyze and identify the target genes of miR-143. Genes with miR-143/miR-NC1 normalized ratios >1.1 were defined as candidates for miR-143 target genes.

Immunohistochemistry. All tumors resected from mouse primary tumors at the right knee joint were fixed with 10% buffered formalin and embedded in paraffin. Sections 3-μm thick were examined using immunohistochemistry. The sections were deparaffinized, and antigens were retrieved by autoclave in 10 mmol/l citrate buffer (pH 6.0) at 121 °C for 10 minutes. Endogenous peroxidase activity was blocked by immersing the slides in 0.6% hydrogen peroxide in methanol for 30 min. The sections were immunostained using a Histofine mouse stain kit (Nichirei, Tokyo, Japan). The primary antibodies used in this study were a mouse monoclonal antibody against human proliferative cell nuclear antigen (1:200; DAKO, Glostrup, Denmark) and a rabbit polyclonal antibody against human MMP-13 antigen (1:2,000; Abcam, Cambridge, UK). Immunoreactions were visualized with diaminobenzidine and the sections were counterstained with hematoxylin.

Western blotting. Western blotting was performed as described previously.[50] The membranes were blotted with a rabbit polyclonal antibody against human MMP-13 antigen (1:2,000; Abcam), or with a monoclonal antibody against β-actin (1:2,000; AC-15; Sigma, St Louis, MO). Signals were visualized with an enhanced chemiluminescence system (ECL Detection System; Amersham Pharmacia Biotech).

Statistical analyses. Statistical analyses were conducted using Student's *t*-test for *in vitro* screening of cell invasion and proliferation, and also to evaluate lung metastasis in an *in vivo* assay, and Welch's *t*-test was used for miR-143 expression analysis using clinical samples. $P < 0.05$ was considered significant.

SUPPLEMENTARY MATERIAL

Figure S1. Expression level of miR-143 in human osteosarcoma cell lines, 143B and HOS.
Figure S2. Effect of miRNA transfection for cell proliferation.
Figure S3. Spontaneous lung metastasis of osteosarcoma mouse model.
Figure S4. miR-143 does not effect to tumor growth in *in vivo*.
Figure S5. Six miR-143 candidate protein expression were down-regulated by miR-143 transfection in 143B.
Figure S6. No effect to expression of KRAS and ERK5 protein by miR-143 in 143B.
Table S1. Seventy-eight genes commonly detected by Ago2 IP and LAMP.
Table S2. Six candidates of miR-143 target genes.

ACKNOWLEDGMENTS

We thank Ms Ayako Inoue and Ms Ayano Matsumoto for their excellent technical assistance. The authors thank KOKEN for providing atelocollagen. This work was supported in-part by a Grant-in-Aid for the Third-Term Comprehensive 10-Year Strategy for Cancer Control, a Grant-in-Aid for Scientific Research on Priority Areas Cancer and Grant-in-Aid for Young Scientists (B) (21791395) in the Ministry of Education, Culture, Sports, Science and Technology, and the Program for Promotion of Fundamental Studies in Health Sciences of the National Institute of Biomedical Innovation (NiBio), and a Takeda Science Foundation.

REFERENCES

1. Link, MP (1993). Osteosarcoma in adolescents and young adults: new developments and controversies. Commentary on the use of presurgical chemotherapy. *Cancer Treat Res* **62**: 383–385.
2. Dorfman, HD and Czerniak, B (1995). Bone cancers. *Cancer* **75**(1 Suppl): 203–210.
3. Provisor, AJ, Ettinger, LJ, Nachman, JB, Krailo, MD, Makley, JT, Yunis, EJ *et al.* (1997). Treatment of nonmetastatic osteosarcoma of the extremity with preoperative and postoperative chemotherapy: a report from the Children's Cancer Group. *J Clin Oncol* **15**: 76–84.
4. Bacci, G, Ferrari, S, Bertoni, F, Ruggieri, P, Picci, P, Longhi, A *et al.* (2000). Long-term outcome for patients with nonmetastatic osteosarcoma of the extremity treated at the istituto ortopedico rizzoli according to the istituto ortopedico rizzoli/osteosarcoma-2 protocol: an updated report. *J Clin Oncol* **18**: 4016–4027.
5. Rytting, M, Pearson, P, Raymond, AK, Ayala, A, Murray, J, Yasko, AW *et al.* (2000). Osteosarcoma in preadolescent patients. *Clin Orthop Relat Res* : 39–50.
6. Ferguson, WS and Goorin, AM (2001). Current treatment of osteosarcoma. *Cancer Invest* **19**: 292–315.
7. Pasquinelli, AE, Reinhart, BJ, Slack, F, Martindale, MQ, Kuroda, MI, Maller, B *et al.* (2000). Conservation of the sequence and temporal expression of let-7 heterochronic regulatory RNA. *Nature* **408**: 86–89.
8. Bartel, DP (2004). MicroRNAs: genomics, biogenesis, mechanism, and function. *Cell* **116**: 281–297.
9. Lewis, BP, Burge, CB and Bartel, DP (2005). Conserved seed pairing, often flanked by adenosines, indicates that thousands of human genes are microRNA targets. *Cell* **120**: 15–20.
10. Lu, J, Getz, G, Miska, EA, Alvarez-Saavedra, E, Lamb, J, Peck, D *et al.* (2005). MicroRNA expression profiles classify human cancers. *Nature* **435**: 834–838.
11. Volinia, S, Calin, GA, Liu, CG, Ambs, S, Cimmino, A, Petrocca, F *et al.* (2006). A microRNA expression signature of human solid tumors defines cancer gene targets. *Proc Natl Acad Sci USA* **103**: 2257–2261.
12. Calin, GA, Ferracin, M, Cimmino, A, Di Leva, G, Shimizu, M, Wojcik, SE *et al.* (2005). A MicroRNA signature associated with prognosis and progression in chronic lymphocytic leukemia. *N Engl J Med* **353**: 1793–1801.
13. Jiang, J, Gusev, Y, Aderca, I, Mettler, TA, Nagorney, DM, Brackett, DJ *et al.* (2008). Association of MicroRNA expression in hepatocellular carcinomas with hepatitis infection, cirrhosis, and patient survival. *Clin Cancer Res* **14**: 419–427.
14. Cimmino, A, Calin, GA, Fabbri, M, Iorio, MV, Ferracin, M, Shimizu, M *et al.* (2005). miR-15 and miR-16 induce apoptosis by targeting BCL2. *Proc Natl Acad Sci USA* **102**: 13944–13949.
15. Meng, F, Henson, R, Wehbe-Janek, H, Ghoshal, K, Jacob, ST and Patel, T (2007). MicroRNA-21 regulates expression of the PTEN tumor suppressor gene in human hepatocellular cancer. *Gastroenterology* **133**: 647–658.
16. Asangani, IA, Rasheed, SA, Nikolova, DA, Leupold, JH, Colburn, NH, Post, S *et al.* (2008). MicroRNA-21 (miR-21) post-transcriptionally downregulates tumor suppressor Pdcd4 and stimulates invasion, intravasation and metastasis in colorectal cancer. *Oncogene* **27**: 2128–2136.
17. Osaki, M, Takeshita, F and Ochiya, T (2008). MicroRNAs as biomarkers and therapeutic drugs in human cancer. *Biomarkers* **13**: 658–670.

18. Fontana, L, Fiori, ME, Albini, S, Cifaldi, L, Giovinazzi, S, Forloni, M *et al.* (2008). Antagomir-17-5p abolishes the growth of therapy-resistant neuroblastoma through p21 and BIM. *PLoS ONE* **3**: e2236.
19. Si, ML, Zhu, S, Wu, H, Lu, Z, Wu, F and Mo, YY (2007). miR-21-mediated tumor growth. *Oncogene* **26**: 2799–2803.
20. Ma, L, Reinhardt, F, Pan, E, Soutschek, J, Bhat, B, Marcusson, EG *et al.* (2010). Therapeutic silencing of miR-10b inhibits metastasis in a mouse mammary tumor model. *Nat Biotechnol* **28**: 341–347.
21. Akao, Y, Nakagawa, Y, Kitade, Y, Kinoshita, T and Naoe, T (2007). Downregulation of microRNAs-143 and -145 in B-cell malignancies. *Cancer Sci* **98**: 1914–1920.
22. Crawford, M, Brawner, E, Batte, K, Yu, L, Hunter, MG, Otterson, GA *et al.* (2008). MicroRNA-126 inhibits invasion in non-small cell lung carcinoma cell lines. *Biochem Biophys Res Commun* **373**: 607–612.
23. Valastyan, S, Reinhardt, F, Benaich, N, Calogrias, D, Szász, AM, Wang, ZC *et al.* (2009). A pleiotropically acting microRNA, miR-31, inhibits breast cancer metastasis. *Cell* **137**: 1032–1046.
24. Tazawa, H, Tsuchiya, N, Izumiya, M and Nakagama, H (2007). Tumor-suppressive miR-34a induces senescence-like growth arrest through modulation of the E2F pathway in human colon cancer cells. *Proc Natl Acad Sci USA* **104**: 15472–15477.
25. Luu, HH, Kang, Q, Park, JK, Si, W, Luo, Q, Jiang, W *et al.* (2005). An orthotopic model of human osteosarcoma growth and spontaneous pulmonary metastasis. *Clin Exp Metastasis* **22**: 319–329.
26. Peltier, HJ and Latham, GJ (2008). Normalization of microRNA expression levels in quantitative RT-PCR assays: identification of suitable reference RNA targets in normal and cancerous human solid tissues. *RNA* **14**: 844–852.
27. Calin, GA and Croce, CM (2006). MicroRNA signatures in human cancers. *Nat Rev Cancer* **6**: 857–866.
28. Ochiya, T, Takahama, Y, Nagahara, S, Sumita, Y, Hisada, A, Itoh, H *et al.* (1999). New delivery system for plasmid DNA *in vivo* using atelocollagen as a carrier material: the Minipellet. *Nat Med* **5**: 707–710.
29. Takeshita, F, Minakuchi, Y, Nagahara, S, Honma, K, Sasaki, H, Hirai, K *et al.* (2005). Efficient delivery of small interfering RNA to bone-metastatic tumors by using atelocollagen in vivo. *Proc Natl Acad Sci USA* **102**: 12177–12182.
30. Takeshita, F, Patrawala, L, Osaki, M, Takahashi, RU, Yamamoto, Y, Kosaka, N *et al.* (2010). Systemic delivery of synthetic microRNA-16 inhibits the growth of metastatic prostate tumors via downregulation of multiple cell-cycle genes. *Mol Ther* **18**: 181–187.
31. Cho, WC (2007). OncomiRs: the discovery and progress of microRNAs in cancers. *Mol Cancer* **6**: 60.
32. Ma, L, Teruya-Feldstein, J and Weinberg, RA (2007). Tumour invasion and metastasis initiated by microRNA-10b in breast cancer. *Nature* **449**: 682–688.
33. Tavazoie, SF, Alarcón, C, Oskarsson, T, Padua, D, Wang, Q, Bos, PD *et al.* (2008). Endogenous human microRNAs that suppress breast cancer metastasis. *Nature* **451**: 147–152.
34. Suzuki, HI, Yamagata, K, Sugimoto, K, Iwamoto, T, Kato, S and Miyazono, K (2009). Modulation of microRNA processing by p53. *Nature* **460**: 529–533.
35. Kent, OA, Chivukula, RR, Mullendore, M, Wentzel, EA, Feldmann, G, Lee, KH *et al.* (2010). Repression of the miR-143/145 cluster by oncogenic Ras initiates a tumor-promoting feed-forward pathway. *Genes Dev* **24**: 2754–2759.
36. Michael, MZ, O' Connor, SM, van Holst Pellekaan, NG, Young, GP and James, RJ (2003). Reduced accumulation of specific microRNAs in colorectal neoplasia. *Mol Cancer Res* **1**: 882–891.
37. Porkka, KP, Pfeiffer, MJ, Waltering, KK, Vessella, RL, Tammela, TL and Visakorpi, T (2007). MicroRNA expression profiling in prostate cancer. *Cancer Res* **67**: 6130–6135.
38. Lui, WO, Pourmand, N, Patterson, BK and Fire, A (2007). Patterns of known and novel small RNAs in human cervical cancer. *Cancer Res* **67**: 6031–6043.
39. Iorio, MV, Visone, R, Di Leva, G, Donati, V, Petrocca, F, Casalini, P *et al.* (2007). MicroRNA signatures in human ovarian cancer. *Cancer Res* **67**: 8699–8707.
40. Chen, X, Guo, X, Zhang, H, Xiang, Y, Chen, J, Yin, Y *et al.* (2009). Role of miR-143 targeting KRAS in colorectal tumorigenesis. *Oncogene* **28**: 1385–1392.
41. Tome, Y, Tsuchiya, H, Hayashi, K, Yamauchi, K, Sugimoto, N, Kanaya, F *et al.* (2009). *In vivo* gene transfer between interacting human osteosarcoma cell lines is associated with acquisition of enhanced metastatic potential. *J Cell Biochem* **108**: 362–367.
42. Stokes, A, Joutsa, J, Ala-Aho, R, Pitchers, M, Pennington, CJ, Martin, C *et al.* (2010). Expression profiles and clinical correlations of degradome components in the tumor microenvironment of head and neck squamous cell carcinoma. *Clin Cancer Res* **16**: 2022–2035.
43. Hsu, CP, Shen, GH and Ko, JL (2006). Matrix metalloproteinase-13 expression is associated with bone marrow microinvolvement and prognosis in non-small cell lung cancer. *Lung Cancer* **52**: 349–357.
44. Corte, MD, Gonzalez, LO, Corte, MG, Quintela, I, Pidal, I, Bongera, M *et al.* (2005). Collagenase-3 (MMP-13) expression in cutaneous malignant melanoma. *Int J Biol Markers* **20**: 242–248.
45. Huang, MY, Chang, HJ, Chung, FY, Yang, MJ, Yang, YH, Wang, JY *et al.* (2010). MMP13 is a potential prognostic marker for colorectal cancer. *Oncol Rep* **24**: 1241–1247.
46. Jenkins, DE, Oei, Y, Hornig, YS, Yu, SF, Dusich, J, Purchio, T *et al.* (2003). Bioluminescent imaging (BLI) to improve and refine traditional murine models of tumor growth and metastasis. *Clin Exp Metastasis* **20**: 733–744.
47. Berlin, O, Samid, D, Donthineni-Rao, R, Akeson, W, Amiel, D and Woods, VL Jr (1993). Development of a novel spontaneous metastasis model of human osteosarcoma transplanted orthotopically into bone of athymic mice. *Cancer Res* **53**: 4890–4895.
48. Miretti, S, Roato, I, Taulli, R, Ponzetto, C, Cilli, M, Olivero, M *et al.* (2008). A mouse model of pulmonary metastasis from spontaneous osteosarcoma monitored *in vivo* by Luciferase imaging. *PLoS ONE* **3**: e1828.
49. Hsu, RJ, Yang, HJ and Tsai, HJ (2009). Labeled microRNA pull-down assay system: an experimental approach for high-throughput identification of microRNA-target mRNAs. *Nucleic Acids Res* **37**: e77.
50. Hayashi, H, Tatebe, S, Osaki, M, Goto, A, Sato, K and Ito, H (1998). Anti-Fas antibody-induced apoptosis in human colorectal carcinoma cell lines: role of the p53 gene. *Apoptosis* **3**: 431–437.

Cancers **2011**, *3*, 1311-1328; doi:10.3390/cancers3011311

OPEN ACCESS

cancers

ISSN 2072-6694
www.mdpi.com/journal/cancers

Review

Cancer Stem Cells in Breast Cancer

Ryou-u Takahashi [1], Fumitaka Takeshita [1], Tomohiro Fujiwara [1,2], Makiko Ono [1] and Takahiro Ochiya [1,*]

[1] Division of Molecular and Cellular Medicine, National Cancer Center Research Institute, 1-1, Tsukiji 5-chome, Chuo-ku, Tokyo 104-0045, Japan; E-Mails: rytakaha@ncc.go.jp (R.T.); futakesh@ncc.go.jp (F.T.); tofujiwa@ncc.go.jp (T.F.); makono@ncc.go.jp (M.O.)

[2] Department of Orthopedic Surgery, Okayama University Graduate School of Medicine, Dentistry, and Pharmaceutical Sciences, Okayama, Japan, 2-5-1 Shikata-cho, Okayama City, Okayama 700-8558, Japan

* Author to whom correspondence should be addressed; E-Mail: tochiya@ncc.go.jp; Tel.: +81-3-3542-2511 ext. 4800; Fax: +81-3-5565-0727.

Received: 17 February 2011; in revised form: 3 March 2011 / Accepted: 11 March 2011 / Published: 15 March 2011

Abstract: The cancer stem cell (CSC) theory is generally acknowledged as an important field of cancer research, not only as an academic matter but also as a crucial aspect of clinical practice. CSCs share a variety of biological properties with normal somatic stem cells in self-renewal, the propagation of differentiated progeny, the expression of specific cell markers and stem cell genes, and the utilization of common signaling pathways and the stem cell niche. However, CSCs differ from normal stem cells in their chemoresistance and their tumorigenic and metastatic activities. In this review, we focus on recent reports regarding the identification of CSC markers and the molecular mechanism of CSC phenotypes to understand the basic properties and molecular target of CSCs. In addition, we especially focus on the CSCs of breast cancer since the use of neoadjuvant chemotherapy can lead to the enrichment of CSCs in patients with that disease. The identification of CSC markers and an improved understanding of the molecular mechanism of CSC phenotypes should lead to progress in cancer therapy and improved prognoses for patients with cancer.

Keywords: cancer stem cells; breast cancer; EMT; TGF-β; microRNAs

---

1. Introduction

To overcome problems related to conventional cancer therapy, many cancer researchers focus on tumor-initiating cells (TICs) or cancer stem cells (CSCs). The term CSC is frequently used to mean TIC. Although the CSC theory is well established and widely accepted [1-4], some controversies remain. CSCs, like normal stem cells, show asymmetric cell division [5,6], chemoresistance [7], and tumorigenicity [5]. CSCs have the capacity to form secondary/tertiary tumors upon serial xenotransplantation into immunodeficient rodents and show the same features as the original tumors. The demonstration of these three capacities, the gold standard for the evaluation of CSC phenotypes, reflects the malignancy of tumors and is critical in cancer therapy. Recent studies have demonstrated that CSCs show metastatic ability. In this article, we discuss the general features of CSCs and focus on their characteristics in breast cancers, in which the identification and analysis of CSC markers and CSC phenotypes are well refined.

2. Origin of Cancer Stem Cells

The development of fluorescent antibodies, flow cytometry, and associated cell sorting has facilitated the identification of the cell population that initiates tumors [5,6]. Furthermore, the development of mouse strains with profound immunodeficiencies has allowed the evaluation of tumor formation ability. With these developing tools, Dick and colleagues demonstrated that, in human acute myeloid leukemia (AML), a rare malignant cell showed the ability to repopulate the entire original disease over several transplantations and that such a cell population existed within the immature $CD34^+CD38^-$, and not the $CD34^+CD38^+$, sub-population [6]. Because of the similarity between $CD34^+CD38^-$ cells and normal hematopoietic stem cells (HSCs), the origin of the cell population in which the disease arises was thought to be this normal population. Subsequent work with colony-formation assay and lentivirus vector tracking identified the cell population that was able to repopulate the disease not only over several transplantations but also over a single transplantation as quiescent stem cells [8]. This hierarchy, which closely mimics the normal process of hematopoietic precursor development, may explain the CSC biology of childhood AML [8].

3. Solid Tumor CSCs

The first solid CSCs were identified in breast tumors in 2003 [5]; subsequently, CSCs have been identified in brain [9,10], colon [11,12], melanoma [13,14], pancreatic [15,16], prostate [17], ovarian [18], hepatic [19], lung [20], and gastric cancers [21]. In breast cancer, $CD44^+$ $CD24^{-/low}$ ESA^+ (epithelial surface antigen, also known as EpCAM) cells were identified as CSCs in a number of solid malignancies [5,22]. These cells are thought to share stem cell-like properties because they are capable of reconstituting the heterogeneity of the original primary tumors. The same approach was used for brain tumors exhibiting a subpopulation of $CD133^+$ cells with CSC phenotypes [9,10]. $CD133^+$ CSCs were subsequently isolated from colon and pancreatic cancers [23,24]. Recently, in hepatocellular carcinoma, EpCAM was identified as a CSC marker and found to be expressed in normal epithelial progenitor cells [25]. Furthermore, aldehyde dehydrogenase (ALDH) is a CSC marker in breast

cancers [26]. The representative cell surface markers for human hematologic and solid cancers reported to date are listed in Table 1.

Table1. Representative Cell Surface Markers for Human Cancer Stem Cells (CSCs).

Cancer Type	Cell Surface Markers	Ref.
AML	$CD34^+CD38^-$	[6]
Breast Cancer	$ESA^+/CD44^+/CD24^{-/low}$	[5]
	ALDH1	[26]
Glioma	CD133	[9,10]
Colon Cancer	CD133	[11,12]
Metastatic Colon Cancer	$CD133^+/CD26^+$	[27]
Melanoma	CD20	[13]
	CD271	[14]
Pancreatic Cancer	$ESA^+/CD44^+/CD24^+$	[16]
Metastatic Pancreatic Cancer	$CD133^+/CXCR4^+$	[15]
Prostate Cancer	$CD44^+/\alpha_2\beta_1{}^+/CD133^+$	[17]
Ovarian Cancer	$CD44^+/CD117^+$	[28]
	$CD44^+/MYD88^+$	[29]
Hepatic Cancer	EpCAM	[25]
Lung Cancer	CD133	[20]
Gastric Cancer	CD44	[21]

AML: Acute myeloid leukemia; CXCR4: Chemokine receptor 4; ESA: Epithelial surface antigen; ALDH: Aldehyde dehydrogenase 1A1; $\alpha_2\beta_1$: Integrin $\alpha_2\beta_1$; MYD88: Myeloid differentiation primary response protein Myd88

4. CSC Markers

4.1. Side Population

Following the identification of the Hoechst 33342 dye-efflux side population (SP) in bone marrow cells in mice as hematopoietic stem cells [30,31], SP cells with stem cell-like properties have been identified in a variety of human hematologic cells and solid malignant cells. These cells show CSC phenotypes characterized by asymmetric cell division, drug resistance, and tumorigenicity [16,32-34]. Thus, SP cells can be assumed to play important roles in CSC fractions. Zhou et al. demonstrated that the expression of the *ABCG2* gene, a member of the ATP binding cassette (ABC) transporter superfamily, is an important determinant of the SP phenotype [35].

A recent study pointed out the following problems in using SP cells as a CSC fraction [36]. First, cells resistant to Hoechst 33342 dye do not necessarily show tumorigenicity and metastatic ability as CSCs. For example, ABCG2-positive MCF-7 cells showed no more tumorigenic potential than did ABCG2-negative cells [37]. Second, the staining condition, staining time, and cellular concentration of Hoechst dye affect the viability of the SP fraction [36]. Third, cytometry gating strategies used to isolate SP cells lack the consistency of gating strategies used in marker staining [36]. These problems latently lead to cross-contamination of the SP and the non-SP fractions, resulting in controversial data.

4.2. CD34

CD34 is a monomeric cell-surface antigen with a molecular mass of approximately 110 kD [6]. In common acute lymphoblastic leukemia (CALL), the expression of CD34 is positively correlated with CD10, known as common acute lymphocytic leukemia antigen (CALLA) [38]. CD34-positive leukemic cells are thought to be a less-differentiated phenotype than CD34-negative cells [6]. CD10 is a key element in the niche that maintains the progenitor and stem cell pools in the mammary lineage [39].

4.3. CD44

CD44 is a useful marker for collecting CSCs not only in breast tumors but also in a variety of other tumor models [5,40,41]. CD44 may also be important in metastasis. Through the implantation of patient tumors or breast CSCs into mouse mammary fat pads and the use of noninvasive imaging strategies, it was demonstrated that $CD44^+$ cells from both primary tumors and lung metastases showed high tumorigenicity [42]. In addition, CD44 variant isoforms are differentially expressed during pregnancy and involution, indicating a role in normal breast epithelial homeostasis [43]. p53 inhibits the expression of the CD44 cell-surface molecule via binding to a noncanonical p53-binding sequence in the CD44 promoter [44]. This interaction enables an untransformed cell to respond to stress-induced, p53-dependent cytostatic and apoptotic signals that would otherwise be blocked by the actions of CD44 [44].

4.4. CD133

As shown in Table 1, recent studies have demonstrated that CD133 (prominin-1) is a specific marker of CSCs in a wide spectrum of malignant tumors [10,12,24]. CD133 was the first identified member of the prominin family of the 5-transmembrane glycoprotein [45]. In 1997, Yin et al. produced a novel monoclonal antibody (MAb) that recognized the AC133 antigen [46], a glycosylation-dependent epitope of CD133, and the expression of AC133 restricted in $CD34^+$ progenitor cells from adult blood [47]. CD133 cDNA encodes a 5-transmembrane domain molecule with an extracellular N-terminus, a cyotoplasmic C-terminus, and two large extracellular loops with eight consensus sites for *N*-linked glycosylation [48]. The characteristic feature of CD133 is its rapid downregulation during cell differentiation [49]. This feature makes CD133 a unique cell surface marker for the identification and isolation of stem cells and progenitor cells in several tissues [45]. According to the CSC theory, CSCs express some stem cell markers as normal stem cells [1,2]. Therefore, tumor cells expressing CD133 independently or in combination with other stem or progenitor cell markers are thought to represent CSCs.

4.5. Aldehyde Dehydrogenase (ALDH)

ALDH1 is a detoxifying enzyme responsible for the oxidation of intracellular aldehydes [50]. ALDH has been reported to have a role in the early differentiation of stem cells in the oxidization of retinol to retinoic acid [51,52]. Furthermore, high ALDH activity has been observed in murine and human hematopoietic and neural stem and progenitor cells [53,54]. An increase in ALDH activity has also been found in stem cell populations in multiple myeloma and AML [55]. Therefore, ALDH

activity may provide a common marker for both normal and malignant stem and progenitor cells. In several tumors, the measurement of ALDH activity is a useful approach in the identification and isolation of CSCs [56-59]. However, the ALDEFLUOR assay does have some limitations in the isolation of the most tumorigenic population, notably in tumors of different origins. For example, both ALDEFLUOR (bright) and ALDEFLUOR (low) from the melanoma cell line were able to initiate tumors after inoculation into NOD/SCID mice [60]. Moreover, tumors generated from ALDEFLUOR (low) cells grew faster and bigger than tumors from ALDEFLUOR (bright), even among passages. These results suggest that the ALDEFLUOR-positive population in melanoma is not stem cell-enriched, unlike the ALDEFLUOR-negative population [60]. Furthermore, the stem cell population identified using the ALDEFLUOR assay is probably heterogeneous and needs to be dissected using additional markers.

4.6. microRNA

Despite progress in the identification of CSC markers, the CSC theory has been complicated by a lack of clearly defined developmental surface markers specific for individual tumor types, making the molecular mechanism of common phenotypes in CSC fractions the object of much ongoing research. In this regard, microRNAs (miRNAs), as a part of non-coding RNA, are considered to be novel markers for CSCs, as shown in Table 2.

Table 2. miRNAs Regulate the CSC Phenotypes.

Cancer Type	microRNA	Potential Targets	Ref.
Breast Cancer	let-7	H-Ras and HMGA2	[61]
	miR-200c	BMI1	[62]
	let-7	IL-6	[63]
	miR-200b	Suz12	[64]
Glioblastoma	miR-199b-5p	HES1	[65]
	miR-34a	c-Met, Notch1, and Notch2	[66]
	miR-328	ABCG2	[67]
Medulloblastoma	miR128a	BMI1	[68]
Hepatic Cancer	miR-181	CDX2, GATA6, and NLK	[69]
Pancreatic Cancer	miR-34s	Bcl2 and Notch	[70]
Osteosarcoma and	miR-140	HDAC4	[71]
Colon Cancer	miR-215	DHFR and Thymidylate synthase	[72]

HMGA2: High mobility group AT-hook2; BMI1: BMI1 Polycomb ring finger oncogene; IL-6: Interleukin 6; SUZ12: Suppressor of zest 12 homolog; HES1: Hairy and enhancer of split 1; CDX2: Caudal type homeobox 2; GATA6: Gata binding protein 6; NLK: Nemo-like kinase 6; HDAC4: Histone deacetylase 4; DHFR: Dihydrofolate reductase

5. Breast Cancer Stem Cells (BCSCs)

5.1. Identification of BCSCs

The pioneering study by Clarke and colleagues used breast cancer xenografts to isolate a population of cells able to initiate tumors in NOD/SCID mice [5]. This population was defined by the combined

expression of the cell surface marker $CD44^+/CD24^{-/low}/lin^-$. As few as 200 of these cells generated tumors in NOD/SCID mice, whereas 20,000 cells that did not display this phenotype failed to do so. The NOD/SCID tumors recapitulated the entire heterogeneity of the initial tumor. Furthermore, the $CD44^+/CD24^{-/low}/lin^-$ cell population was able to reinitiate tumors in NOD/SCID mice and retained this ability after serial passages. Thus, these cells, which had the ability to self-renew and to differentiate and which displayed tumorigenic capacity, had CSC features.

Through the use of the $CD44^+/CD24^{-/low}/lin^-$ phenotype and another marker, the ALDEFLUOR assay, it has been shown that cells able to initiate tumors in mice are among the ALDEFLUOR-positive cells, the cells displaying both phenotypes being the most tumorigenic, and that none of the $CD44^+/CD24^{-/low}/lin^-$ cells without ALDEFLUOR activity can grow in mice [26]. These results indicate that the $CD44^+/CD24^{-/low}/lin^-$ population contains some but not all of the CSCs in breast tumors. Moreover, while CD44 appears to be a common stem cell marker [73-75], as well as a promising therapeutic target [76,77], the $CD44^+/CD24^{-/low}/lin^-$ phenotype is probably tissue restricted. For example, pancreatic cancer cells with stem cell properties of self-renewal, the ability to produce differentiated progeny, and increased expression of the developmental signaling molecule sonic hedgehog display a $CD44^+/CD24^+/ESA^+$ phenotype [16,78].

5.2. Epithelial-Mesenchymal Transition (EMT)

Pathophysiological conditions such as tissue injury or tumorigenesis can trigger differentiated cells to acquire a multipotent stem cell-like phenotype through EMT induction [32,79]. This acquisition may mirror developmentally regulated EMT signaling pathways, such as Wnt, Notch, and Hedgehog, which drive both normal and CSC renewal and maintenance [32,80,81]. Metastatic cancer cells, which have presumably undergone EMT, may exhibit CSC phenotypes. For instance, in murine and human melanoma, cancer metastasis is accelerated through immunosuppression during Snail-induced EMT [82]. A recent study revealed a subpopulation of $CD26^+$ cancer stem cells showing not only chemoresistance but also metastatic potential in human colorectal cancer [27]. In breast tumors, $CD44^+$ cells from both primary tumors and lung metastases are highly enriched for tumor-initiating cells [42].

Empirical evidence connecting EMT to the acquisition of stem cell phenotypes has recently been reported by Weinberg et al. [83]. The differentiated mammary epithelial cells that have undergone EMT either on transforming growth factor beta (TGF-β) treatment or by the expression of E-cadherin transcriptional repressors, such as Snail or Twist, generate $CD44^+/CD24^-$ cells as BCSCs [83]. The same researchers also demonstrated that E-cadherin knockdown generated $CD44^+/CD24^-$ cells showing BCSC properties [7]. In addition, stem cells isolated from normal breast tissue or breast cancers express a number of canonical EMT markers [83]. Of clinical significance, an immune response that induces the EMT-associated emergence of CSCs as $CD8^+$T-cells can induce the dedifferentiation of breast cancer cells, resulting in the generation of $CD44^+/CD24^-$ stem cell-like cells [84]. In summary, accumulating evidence links EMT to the generation of CSC-like phenotypes, which may be prerequisites for cancer cell metastasis.

5.3. TGF-β

TGF-β family cytokines are mediators of embryonic development and tissue homeostasis in adults [85]. TGF-β signaling controls many types of physiological and pathophysiological EMT [79,86]. Type I and type II TGF- β receptors (TβRI and RII, respectively) are dual specificity kinases that possess both serine/threonine and tyrosine kinase activities [87]. TβRI activates effector Smads 2 and 3, which subsequently bind to a co-smad, Smad4. The Smad2, Smad3, and Smad4 complexes can associate with accessory transcription factors to activate the expression of target genes that cause changes in cellular differentiation. Notably, Smads associate with zinc finger E-box binding (ZEB) proteins to repress the expression of E-cadherin during the initiation of EMT [88-91]. TGF-β suppresses tumor growth strongly and induces apoptotic effects during the early stages of tumor progression. However, tumors show that EMT becomes insensitive to TGF-β-mediated growth inhibition while showing increased tumor invasion and metastasis. Significant progress has been made in the elucidation of the cellular and molecular events that regulate tumor-promoting effects on microenvironments and tumor cells. Indeed, in breast cancer, mesenchymal stem cell (MSC)-derived TGF- β1 increases the frequency of regulatory T cells, resulting in the support of breast cancer growth [92]. TGF-β signaling is also reported to regulate the expression and activity of matrix metalloproteases (MMP-2 and MMP-9) and downregulate the expression of the protease inhibitor TIMP in tumor and endothelial cells [93]. Furthermore, recent work has uncovered an intricate new mechanism through which TGF-β acts in concert with oncogenic Ras to antagonize the p63-metastasis protective function [94]. p63 inhibition requires the combined action of Ras-activated mutant p53 and TGFβ-induced Smads, mechanistically involving the formation of a p63-Smads-mutant p53 ternary complex. Remarkably, two of the key downstream targets (*cyclin G2 and SHARP1*) of p63 are prognostic tools for breast cancer metastasis.

5.4. MicroRNAs (miRNAs) in Regulation of BCSCs

The emergence of miRNAs as important players in breast cancer has led researchers to explore the molecular mechanism that regulates BCSC phenotypes [61-63]. Some miRNAs play important roles in the phenotype formation of BCSCs, and multiple targets of these miRNAs have been identified [95,96] (Figure 1). Let-7 was originally identified in the nematode Caenorhabditis elegans [97,98]. Subsequently, the conservation of the let-7 sequence and its function in mammals were reported. Let-7 was one of the most consistently and significantly reduced miRNAs in many types of tumors, and downreglation of its expression was associated with the progression of tumor malignancy [99]. Recent studies have shown that let-7 suppresses self-renewal in both normal cells and BCSCs. Let-7 also regulates BCSC phenotypes such as chemoresistance and asymmetric cell division [61]. Several oncogenes, including c-Myc, Ras, HMGA2, cyclin D, and IL-6, have been reported as the targets of let-7 [61,63,99]. HMGA2 and Ras are highly expressed in BCSCs and remarkably repressed in non-BCSCs [61]. A comprehensive pathway involved in let-7 and lin-28 promotes the tumor metastasis and BCSC-induced inflammatory response [63]. Lin-28 is a highly specific embryonic stem cell marker and behaves as a negative regulator of let-7. Let-7 also directly represses lin-28 expression in ES and cancer cells [100].

In a comparison of the miRNA expression profiles of BCSCs and non-CSCs from human breast tumor samples, some miRNAs were upregulated and downregulated in BCSCs [62]. Three clusters, miR-200c-141, miR-200b-200a-429, and miR-183-96-182, were downregulated in human BCSCs [62]. Further study demonstrated that miR-200c regulated BCSC phenotypes by regulating the expression of BMI1, a member of the polycomb group of proteins, and acted as a negative regulator of stem cell phenotypes such as apoptosis, senescence, and differentiation [62].

miR-9, which is upregulated in breast cancer cells, directly targets CDH1, the E-cadherin-encoding messenger RNA, and also promotes cell motility and invasiveness [101]. miR-9-mediated E-cadherin downregulation results in the activation of beta-catenin signaling, which contributes to the upregulated expression of the gene encoding vascular endothelial growth factor (VEGF), which increases tumor angiogenesis [101]. Expression of miR-9 is activated by MYC and MYCN, both of which directly bind to the mir-9-3 locus. Significantly, in human cancers, miR-9 levels correlate with MYCN amplification, tumor grade, and metastatic status [101].

Thus, the dysregulation of miRNA is responsible for the BCSC phenotypes in the malignant progression of breast cancer, and the elucidation of the precise molecular mechanism may be the next step toward a more complete understanding of the regulatory networks underlying BCSC phenotypes, including metastasis.

Figure 1. miRNA regulates BCSC phenotypes. Let-7 [61], miR-30 [102], and miR-200 [62] may regulate BCSC phenotypes by modulating the expression of their target genes. The expression of let-7, miR-30, and miR-200 is remarkably reduced in BCSCs, progressively increased with the differentiation of BCSCs, and inversely correlated with the expression of their target genes. miR-9 [101], miR-328 [67], miR-373 and miR-520c [103] also regulate BCSC phenotypes.

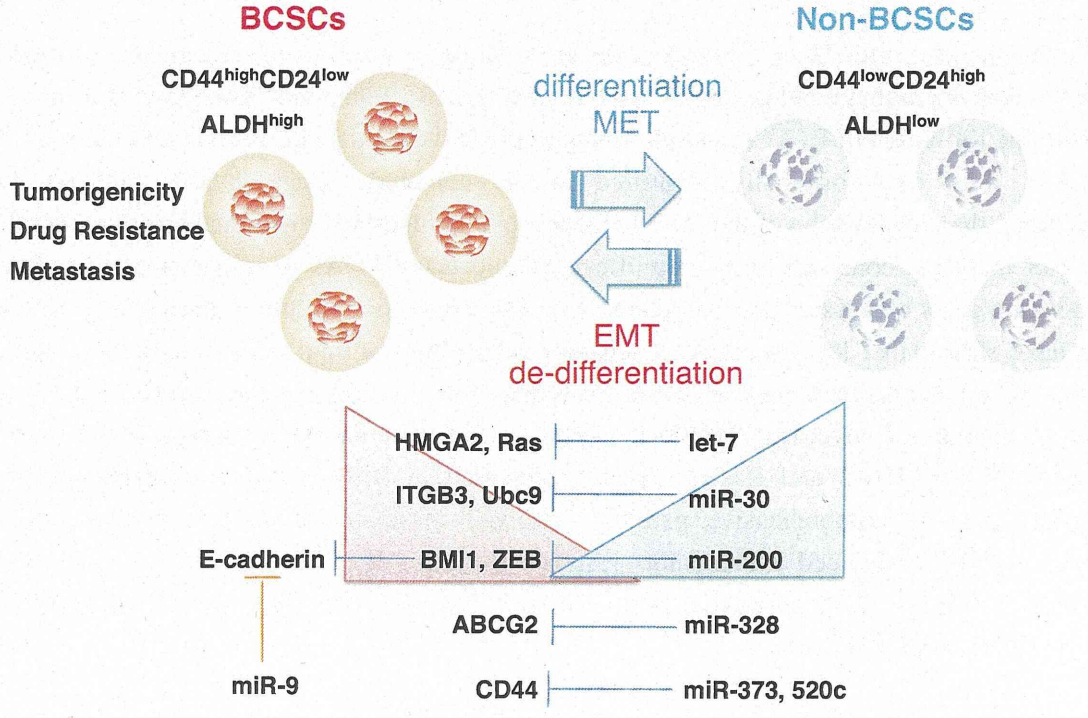

6. CSC-Related Therapy

The development of therapies against CSCs is challenging because both bulk tumor cells and CSCs must be eliminated. As CSCs are molecularly distinct from bulk tumor cells, one can target their activity by exploiting the molecular differences [76,104-107]. For instance, cell surface marker expression could be used for antibody-directed therapy to target proteins, such as CD133, CD44, or ABC transporters, which are ATP-dependent drug efflux pumps [76,104-106]. A recent study identified ribophorin II (RPN2), part of an *N*-oligosaccharyl transferase complex, as a novel regulator of drug resistance via the regulation of the *N*-linked glycosylation of ABCB1 (P-glycoprotein) in breast cancer [107]. The downregulation of RPN2 most efficiently induces apoptosis of drug-resistant breast cancer cells in the presence of docetaxel. However, prior to developing an anti RPN2 therapy against cancer stem cells, the safety of the effect of RPN2 silencing in normal tissue stem cells should be tested.

Another strategy to selectively target CSCs is high-throughput compound screening. In one study, the antibiotic salinomycin preferentially killed BCSCs [7]. Interestingly, salinomycin induced the differentiation of BCSCs *in vivo*, as assessed by increased E-cadherin and reduced vimentin expression [7]. Furthermore, a recent study showed that salinomycin effectively reduced the number of P-glycoprotein expressing cells [108]. The activation of AMP-activated kinase with the diabetes drug metformin also resulted in the selective killing of CSCs in combination with chemotherapy [109]. This finding suggests that targeting mTOR activity, which is negatively regulated by AMP-activated kinase, may be a strategy to block BCSC phenotypes [110,111].

Recent studies have shown that oncolytic viruses seem to be well suited to eliminate CSCs because the viruses are cytotoxic and are not subject to drug efflux such as ABC transporters and defective apoptotic signaling [112]. These viruses are emerging as novel tools for cancer therapy, and several are already in clinical trials [113,114]. Virotherapy can also be utilized to sensitize tumor cells to radiation and chemotherapy and as tools for immunotherapy [115]. Thus, oncolytic viruses have significant advantages for improved treatment options for patients. In breast cancer, capsid-modified adenovirus vectors and reovirus vectors are effective for the elimination of BCSCs [116,117]. A recent study showed that BCSCs had dysregulated innate immune responses caused by impaired trafficking of toll-like receptor 9 (TLR9) and cofactor MyD88 and the absence of TLR2, resulting in dysfunctional virus recognition. These defects induced the dysfunctional induction of the type I interferon (IFN) response in BCSCs, leading to permissivity to the oncolytic adenovirus [118].

7. Conclusions

As accumulating evidence demonstrates that cancers are heterogeneous, clinical oncologists and cancer researchers need to consider which cancer cells have the potential to contribute to disease progression, including drug resistance and metastasis. Moreover, in breast cancer, recent studies have shown that non-CSCs acquire the CSC phenotype through EMT. Several key signaling pathways contribute to this process, namely, TGF-β and Wnt, known inducers of EMT and promoters of stem cell maintenance. The microRNAs also play critical roles in these processes, and the dysregulation of